ICANS XIX,
19th meeting on Collaboration of Advanced Neutron Sources
March 8 – 12, 2010
Grindelwald, Switzerland

PROTON AND NEUTRON PENETRATION OF CANDIDATE TARGET MATERIALS FOR THE EUROPEAN SPALLATION SOURCE

MARY PW CHIN[1, 2]
1) European Spallation Source (ESS), Lund University, P. O. Box 117
SE-22100 Lund, Sweden
2) European Organization for Nuclear Research (CERN), Department EN/STI
CH-1211 Geneva 23, Switzerland

and

CYRIL KHAROUA[1, 2], ETAM NOAH[1, 2], FRANCOIS PLEWINSKI[1], DANIELA ENE[1]

ABSTRACT

Candidate target materials (Hg, PbBi, PbAu, PbMg, liquid Pb and solid W) and beam footprints (Gaussian squares, uniform circulars and doughnuts) are investigated for the European Spallation Source (ESS), to be built in Lund (Sweden), where the first neutron is expected in a decade. Monte Carlo estimations of the magnitude and location of the peak neutron fluence, proton fluence and the competing neutron creation and neutron absorption provide a parallel résumé of different target materials, target dimensions and beam footprints. These data will aid good positioning of the moderators as well as strategic cutting of an adequately-cooled target, which is to survive a best-estimated lifetime.

1. Motivation

The European Spallation Source (ESS) had undergone earlier design phases ([1] and references therein) prior to the recent firm approval. Meanwhile, the mercury target as a (p,xn) neutron source has been realised and is tracing good operational records at the Spallation Neutron Source (SNS) and the Japanese Spallation Neutron Source (JSNS) at ORNL and J-PARC, respectively. The prospects of liquid lead alloys as spallation targets are not new [2]. Building from the wealth of existing knowledge, and as the ESS project gains unprecedented momentum, this work investigates some neutronic aspects of the options available for the spallation target. It complements existing work on 'bare targets' (*e.g.* [3]) by exploring a different set of irradiation conditions, configurations and scorings.

2. Materials and methods

A generic* spallation target was simulated using FLUKA [4] version 2008.3b. The geometry consists of a homogeneous cylinder of 100 cm radius and 200 cm length. 4×10^6

---

* 'generic' in that this study is applicable regardless of whether the target is rotating, circulating or stationary, and is independent of the eventual selected specifications for the complete target-moderator-reflector system.

2.5 GeV primary protons impinge the centre of the base of the cylinder. Quantities are scored (Table I) by radial symmetry. The simulation was repeated with different candidate target materials (Table II) and beam footprints (Table III).

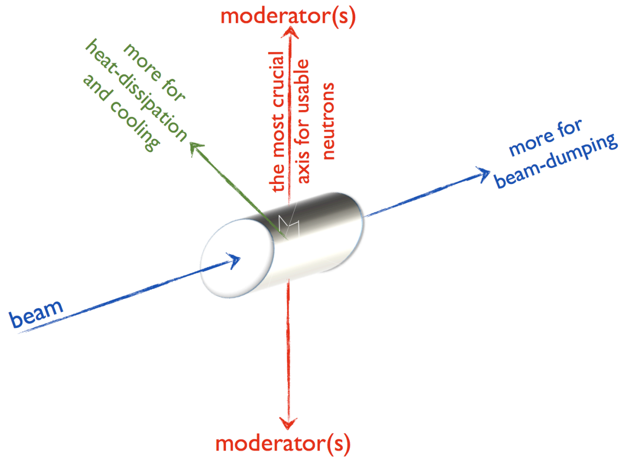

Fig. 1. The three axes of the generic target of a wing-type moderator arrangement, each with its distinct design interest.

Table I. Quantities scored and the corresponding context.

quantity	**context**
Spatially-differentiated proton fluence and neutron fluence	To measure the forward and lateral penetrations in the target; this is among the criteria for selecting the optimal target dimension. Note the distinct design interest for each axes (Fig. 1).
Neutron balance, which is the number of newly-created neutrons minus those absorbed	To complement the information obtained from neutron fluence, to aid our understanding of the local neutron presence.

Table II. Candidate target materials investigated.

material	**relative mass fractions**	**density (g cm^{-3})**
Hg (liquid)	1.000 Hg	13.55
PbBi (LBE)	0.450 Pb, 0.550 Bi	10.50
PbAu	0.850 Pb, 0.150 Au	12.60
PbMg	0.975 Pb, 0.025 Mg	10.60
Pb (liquid)	1.000 Pb	10.70
W (solid)	1.000 W	19.30

3. Results

The proton fluence built up to a maximum in the second centimetre along the beam central axis whereas the neutron fluence built up later, in the fourth centimetre, signifying a supply of secondary neutrons in addition to the (p,xn) spallation process (Fig. 2). The neutron *population* continues to grow (positive gradient on the neutron fluence, Fig. 2b) even as the *death rate* begins to increase with respect to the *birth rate* of newly-created neutrons (negative gradient on the neutron balance, Fig. 2c). Throughout this paper quantities are presented per proton source started; error bars are too small to be visible.

Table III. Beam footprints investigated.

beam footprint	**attributes**
Pencil beam	
Uniform circular beams	radii of 1, 4, 10 and 25 cm

Doughnut beams of outer radius r_{out} and innder radius r_{in}	with r_{out} fixed at 25 cm, r_{in} = 5, 10, 15, 20 and 24 cm;
	with r_{out}-r_{in} fixed at 1 cm, r_{out} = 4 to 22 cm in steps of 3 cm;
	with r_{out}-r_{in} fixed at 4 cm, r_{out} = 14 and 24 cm;
	with r_{out}-r_{in} fixed at 10 cm, r_{out} = 20 and 30 cm

Gaussian square beams	sides of 1 cm to 8 cm in steps of 1 cm

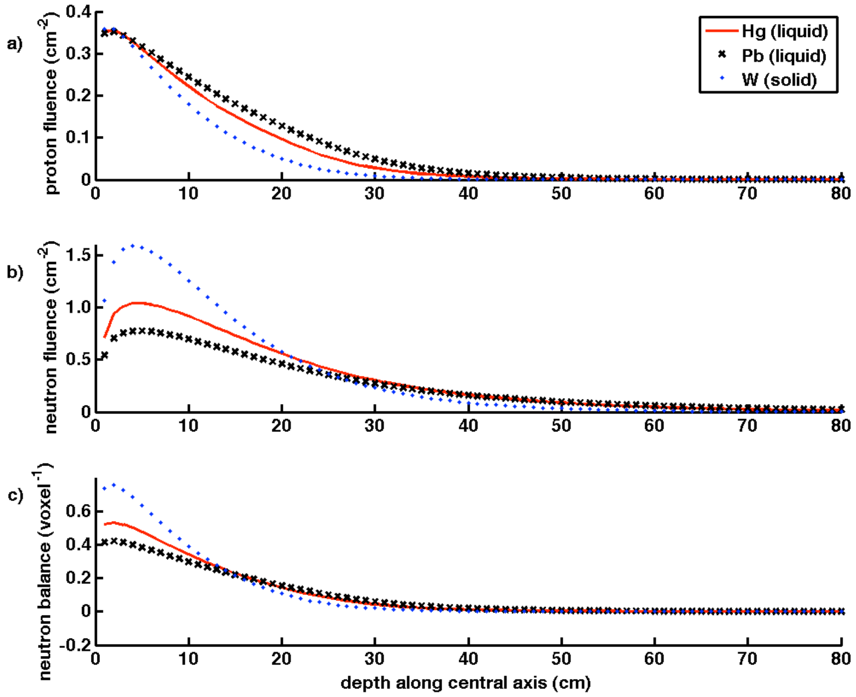

Fig. 2. Proton fluence, neutron fluence and neutron balance along the beam central axis produced by a pencil beam. Note the change from positive to negative gradients for the neutron balance.

For the configurations investigated, it is observed that the smaller the beam the higher the peak neutron fluence (Fig. 3 and Fig. 4). The location of the peak, however, is very much confined to the central axis of the target (Fig. 5). This is at < 1 cm radius for the pencil beam, the uniform circular beams as well as the Gaussian square beams (not plotted). Doughnut beams managed to take this location of the peak further out in the radial/lateral direction (Fig. 5); the magnitude of the peak is, however, considerably reduced (Fig. 1). Larger beam footprints push the depth of peak neutron fluence further (Fig. 7 and Fig. 8); this has important implications on the positioning of the moderator and the possibility of placing two moderators parallel to the beam central axis on the same side of the target.

From the four series of doughnut beams (Table III), results show that for each series the trend is monotonic. Therefore, only data for the extreme points are plotted. This observation suggests that for future design of experiments where additional degrees of freedom are either absent or negligible, the extreme points could be assumed to provide adequate sampling without causing aliasing effects.

The seeming peculiarity in the lateral position of the peak neutron fluence in PbMg by a r_{out}=30 r_{in}=20 doughnut beam (Fig. 5) is confirmed and explained by the 2D distributions plotted in Fig. 6 for PbMg (where r_{out}=30 r_{in}=20 and r_{out}=24 r_{in}=20 results are significantly different) and PbBi (where r_{out}=30 r_{in}=20 and r_{out}=24 r_{in}=20 results are similar).

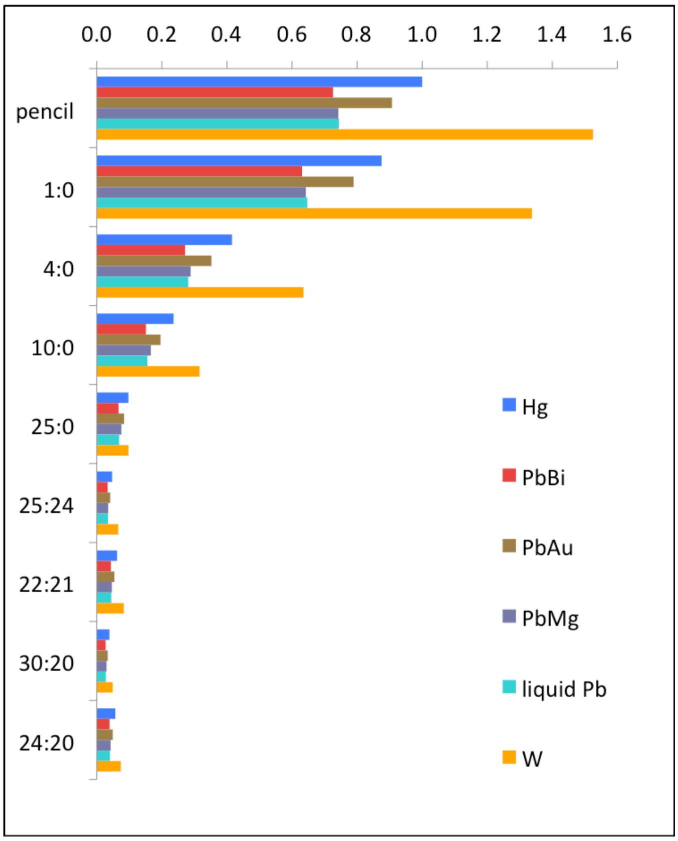

Fig. 3. The peak neutron fluence for pencil, circular and doughnut (labelled as r_{out}:r_{in}) beam footprints. Data have been normalised to that of the pencil beam on Hg.

The neutron penetration (Fig. 2) and the peak neutron fluence (Fig 3 and Fig. 4) are more sensitive to the material types compared to the lateral/radial location of the peak (Fig. 5). In terms of the peak neutron fluence (Fig. 3 and Fig. 4) and its depth (Fig. 7 and Fig. 8), the different materials exhibited predictable trends across the beam footprints investigated, with W being the highest, followed by Hg and PbAu. An interesting feature is that PbAu differs distinctly from PbBi, PbMg and liquid Pb.

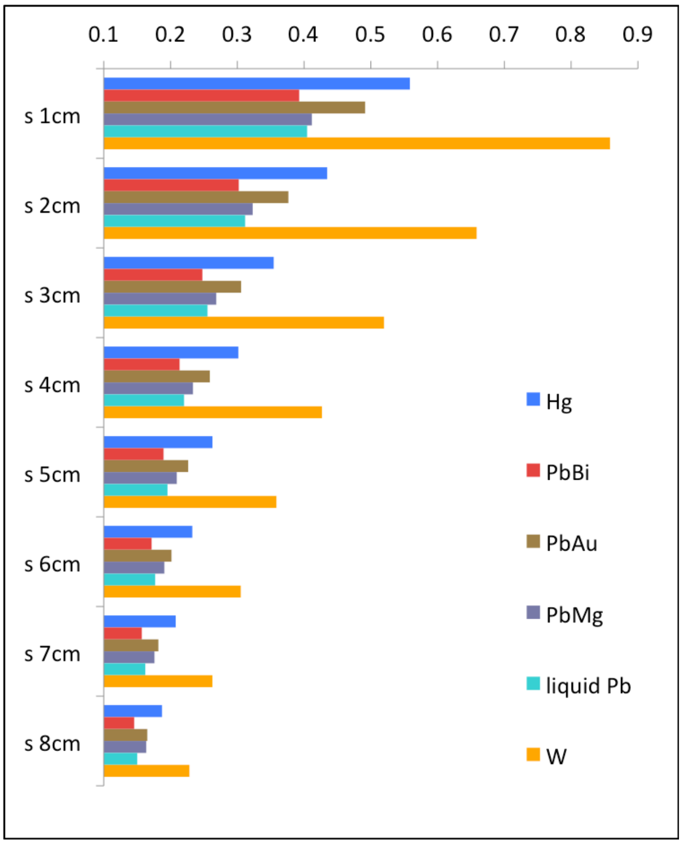

Fig. 4. The peak neutron fluence for Gaussian square beams of sides 1 to 8 cm. Data have been normalised to that of the pencil beam on Hg.

4. Discussion and conclusion

5.1. A slim target?

The location of the maximum neutron fluence being confined to the central axis has major implications. On the one hand, the target should be cut where the neutron fluence is maximum, so as to obtain as many neutrons exiting the target as possible. On the other hand, a spatial spread is typically preferred in terms of heat deposition, cooling and material damage. A crucial quantity is the energy deposition estimated from the same Monte Carlo simulations. This, along with the energy spectra shall be reported separately due to the lack of space.

5.2. Choice of target material

The choice of materials depends considerably on the non-neutronic aspects such as material damage, for which the chemistry is beyond Monte Carlo particle transport codes. For some combinations of materials and irradiation conditions, the damage phenomena are yet to be measured and/or understood. Acknowledging such constraints, neutronic studies are nonetheless warranted by its own right: W is found to provide the most generous source of neutrons, followed by Hg and PbAu.

5.3. Introducing a cavity in the beam footprint

There was a suggestion that perhaps introducing a cavity at the centre, resulting in a doughnut beam footprint, would avoid unnecessary heating and damage at the core of the target if the neutrons produced there were not going to emerge from the target anyway. For the configurations studied here, this has been proven wrong. Nevertheless the data obtained here would facilitate choices if doughnut beams turn out to be a good compromise between neutronics and constraints from heating and material damage.

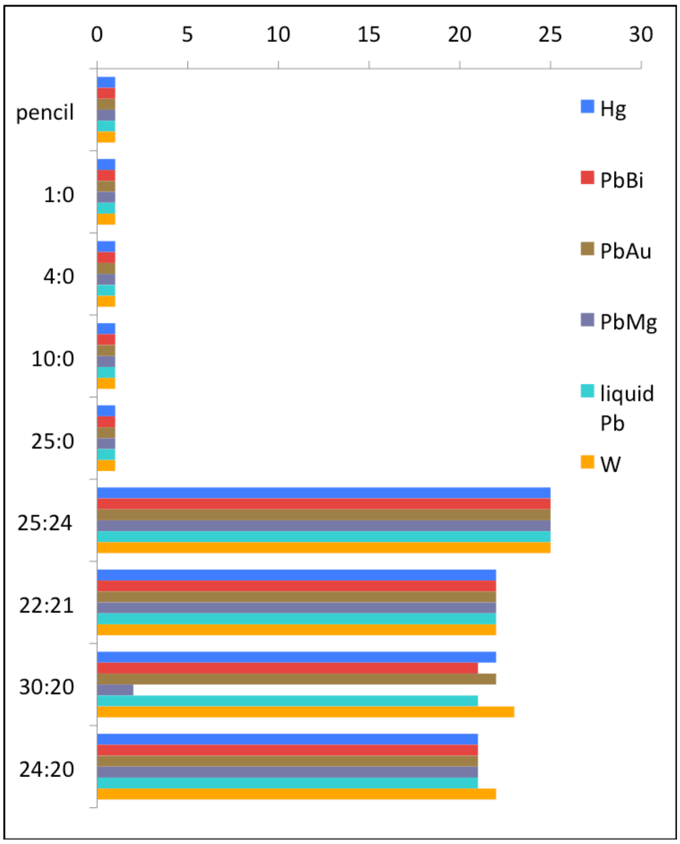

Fig. 5. The lateral position *i.e*. the radius of the cylinder (cm) where the peak neutron fluence occurs: pencil, circular and doughnut (labelled as r_{out}:r_{in}) beam footprints.

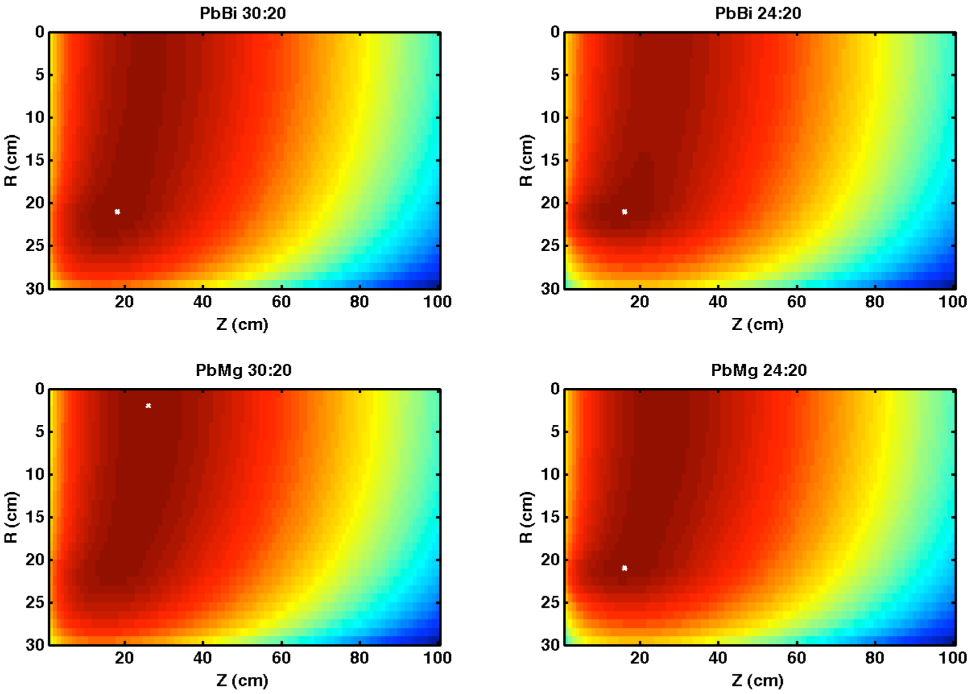

Fig. 6. 2D distribution of neutron fluence along the depth and radial directions for PbBi and PbMg for doughnut beams r_{out}:r_{in}. The white pixel on each marks the point of peak neutron fluence.

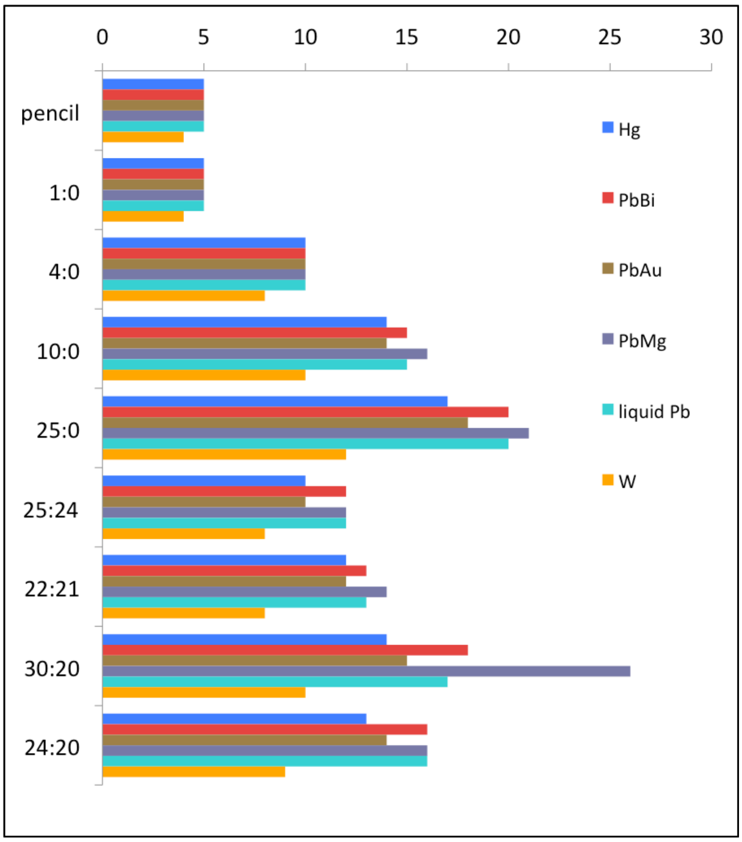

Fig. 7. The depth (cm) where the peak neutron fluence occurs: pencil, circular and doughnut (labelled as r_{out}:r_{in}) beam footprints.

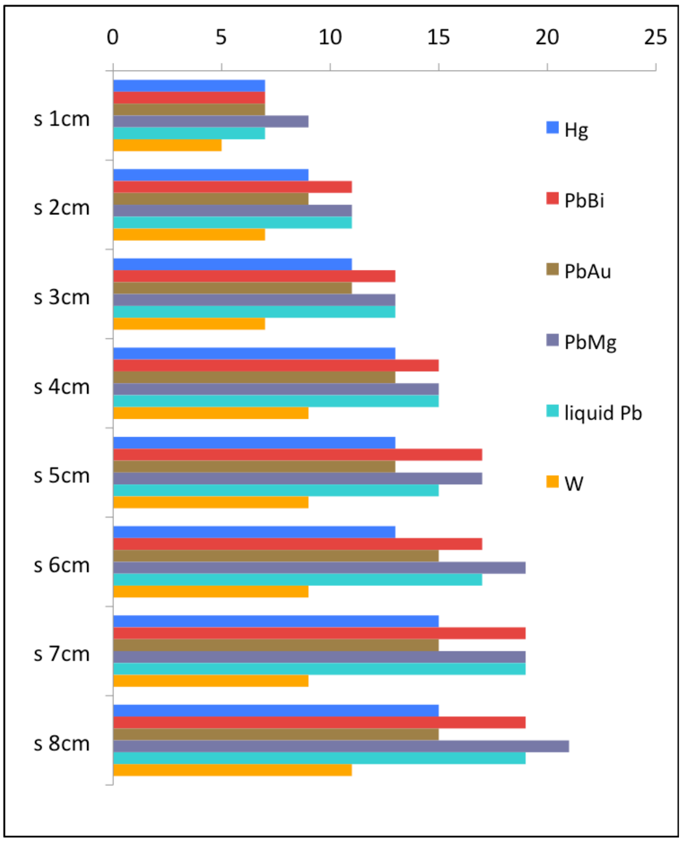

Fig. 8. The depth (cm) where the peak neutron fluence occurs: Gaussian square beams of sides 1 to 8 cm.

5. References

1. *The ESS Project Volume III update,* ISBN 3-89336-345-9 (2003).
2. OECD/NEA, *Handbook on lead-bismuth eutectic alloy and lead properties, materials compatibility, thermal-hydraulics and technologies* (OECD, Paris, 2007).
3. N. Watanabe, *Neutronics of pulsed spallation neutron sources*, Rep. Prog. Phys. **66** (2003) 339-81.
4. A. Ferrari, P.R. Sala, A. Fasso', and J. Ranft, *FLUKA: a multi-particle transport code,* CERN 2005-10, INFN/TC_05/11, SLAC-R-773 (2005).